

## S<sup>4</sup>MC Observations of Dust in the Small Magellanic Cloud Supernova Remnant 1E 0102.2–7219

Karin Sandstrom<sup>1</sup>, Alberto Bolatto<sup>2</sup>, Snežana Stanimirović<sup>3</sup>, J. D. Smith<sup>4</sup> Joshua D. Simon<sup>5</sup> and Adam Leroy<sup>6</sup>

### ABSTRACT

The quantity and composition of dust produced in core-collapse supernovae is a matter of much debate. Observations of dust around quasars at high redshift have been explained via models invoking efficient dust production, with typical yields of 0.1-1  $M_{\odot}$  of dust per supernova. Observations of supernovae and their remnants, however, have yet to provide evidence for efficient dust production. Observations by Stanimirović et al. (2005) of the young, oxygen rich, supernova remnant 1E 0102.2 – 7219 in the Small Magellanic Cloud placed an upper limit on the dust produced in the supernova of  $8 \times 10^{-4} M_{\odot}$ , far less than the amount predicted by models. We present 5-35  $\mu\text{m}$  IRS spectral mapping observations of SNR E 0102 obtained as part of the Spitzer Spectroscopic Survey of the Small Magellanic Cloud (S<sup>4</sup>MC). The spectral information allows us to quantify the contribution of the [O IV] emission line at 25.8  $\mu\text{m}$  to the 24  $\mu\text{m}$  MIPS flux—a major source of uncertainty for Stanimirović et al.—to be  $\sim 10\%$  of the total 24  $\mu\text{m}$  flux. From fits to the spectral continuum we find on the order of  $5 \times 10^{-4} M_{\odot}$  of  $\sim 110$  K dust in the remnant. We compare the spatial distribution of the hot dust continuum with that of the line emission and infer the physical conditions in the remnant. We also discuss the composition of the hot dust as revealed by the infrared spectrum.

---

<sup>1</sup>Department of Astronomy, University of California, Berkeley

<sup>2</sup>Department of Astronomy, University of Maryland, College Park

<sup>3</sup>Department of Astronomy, University of Wisconsin, Madison

<sup>4</sup>Steward Observatory, University of Arizona

<sup>5</sup>Department of Astronomy, California Institute of Technology

<sup>6</sup>Max Planck Institut für Astronomie, Heidelberg Germany

*Subject headings:* galaxies: ISM — infrared: galaxies — infrared: ISM — ISM:  
dust, extinction — ISM: structure

## 1. Introduction

Observations of large dust masses around high redshift quasars highlight a major issue with our understanding of the evolution of dust in the universe. The high redshift of these systems and the large dust masses involved necessitate a short timescale for dust production, a criterion that can only be satisfied by core-collapse supernovae (CCSN) in the current understanding of dust production timescales. They also necessitate efficient dust production by the CCSN. Dwek et al. (2007), for instance, estimate that a dust production of  $\sim 1 M_{\odot}$  per CCSN is necessary to explain the amount of dust around the  $z = 6.42$  quasar SDSS J1148 + 5251. Observations of CCSN and their remnants, however, have yet to provide unambiguous evidence of dust production efficiencies that can account for the high redshift observations.

Detecting newly formed dust in a CCSN or its remnant is observationally challenging for a variety of reasons. In the first few years after the explosion, depending on the brightness of the event, dust may be detected via near- and mid-IR emission (e.g. Wooden et al. 1993) and/or by the extinction effects on the emission line profiles of the expanding supernova ejecta (e.g. Elmhamdi et al. 2003). Recently Sugerman et al. (2006) claimed the detection of  $0.02 M_{\odot}$  of newly formed dust in SN 2003gd based on mid-infrared Spitzer IRAC and MIPS imaging. This claim was subsequently challenged by Meikle et al. (2007) who find evidence for only  $4 \times 10^{-5} M_{\odot}$  of dust from a reanalysis of the IRAC and MIPS data. Issues that interfere with detecting newly formed dust in the first few years after the explosion are light echoes from the circumstellar medium (CSM) (Meikle et al. 2006), clumpiness of the condensed dust (Ercolano et al. 2007), and the difficulty of late time observations of SNe. After the first few years, the ejecta expansion has allowed the newly formed dust to cool to temperatures which make it observable in the far-IR or submillimeter. Observing dust at these wavelengths is very difficult due to complex foregrounds (since CCSN tend to happen near star-forming regions) and low angular resolution. Claims of  $\sim 2 M_{\odot}$  of newly formed dust in Cas A by Dunne et al. (2003) were called into question by Krause et al. (2004) due to the presence of an intervening molecular cloud which complicates the interpretation of the submillimeter observations. After the reverse shock has begun to propagate back into the supernova ejecta, the newly formed dust is heated by collisions with the post-shock plasma and again becomes visible in the mid-IR. Recently, Rho et al. (2008) claimed detection of

$\sim 0.02 M_{\odot}$  of hot dust in Cas A based on mid-IR spectral mapping observations of the remnant. In these proceedings we discuss similar observations of another CCSN remnant, 1E 0102.2 – 7219 in the Small Magellanic Cloud.

SNR 1E 0102.2 – 7219 is a young, oxygen-rich remnant located on the outskirts of the star-forming region N 76. It is thought to be the product of a Type Ib/Ic or IIL/b supernova (Blair et al. 2000, Chevalier 2005) due to the lack of hydrogen and helium in the remnant’s spectrum. The expansion velocity of the remnant is measured to be  $\sim 6000$  km/s by Tuohy & Dopita (1983) and the age of the remnant is  $\sim 1000$  years. E 0102 has been observed extensively at x-ray, UV, optical and radio wavelengths. Stanimirović et al. (2005) presented the first infrared detection of SNR E 0102 from the Spitzer Survey of the Small Magellanic Cloud (S<sup>3</sup>MC) observations. S<sup>3</sup>MC covered the major star-forming regions of the SMC with imaging in all MIPS and IRAC bands (Bolatto et al. 2007). The remnant was only clearly detected at  $24 \mu\text{m}$ . Stanimirović et al. (2005) used the upper limits in the other bands to argue that the dust in the remnant has a temperature of  $\sim 100$  K. They also determined an upper limit of  $8 \times 10^{-4} M_{\odot}$  of dust. In this proceedings we present Spitzer IRS spectral mapping observations of SNR 1E 0102.2 – 7219 obtained as part of the Spitzer Spectroscopic Survey of the Small Magellanic Cloud (S<sup>4</sup>MC). In Section 2 we describe the observations and their reduction. In Section 3 we present the spectrum of the remnant and discuss the spatial distribution of its various components. In Section 4 we present initial results on the mass of newly formed dust in the remnant.

## 2. Observations

E 0102 was mapped using the low-resolution orders of the Infrared Spectrograph (IRS) on the Spitzer Space Telescope (Houck et al. 2004) as part of the S<sup>4</sup>MC project (P.I. Bolatto, GO 30491). The LL and SL orders provide wavelength coverage from 5 to  $38 \mu\text{m}$  with a spectral resolution ranging between  $R \sim 60$  and 120. As a compromise between spatial coverage and sensitivity, ramp times of 14 seconds were used. The maps are fully sampled for both the SL and LL orders. We followed the Spitzer Science Center recommendation of using one-half slit width steps perpendicular to the slit for both SL and LL as well as one-half slit width steps parallel to the slit for LL. For the SL orders we used steps of a full slit width parallel to the slit in order to increase the coverage of the map. Although this technique reduces the redundancy of the SL maps, it has been shown to work well in the SINGS observations. In addition, redundancy is less of a concern in the SL orders compared to the LL orders due to the increasing number of rogue pixels at long wavelengths.

The spectral maps were assembled and calibrated using the Cubism software package

(Smith et al. 2007) in IDL. A designated “off” position was used for removal of Galactic and zodiacal light foregrounds, located at R. A.  $1^{\text{h}}9^{\text{m}}40^{\text{s}}00$  and Dec  $-73^{\circ}31'30''00$  (J2000.0) for both the LL and SL maps. This position was chosen from the S<sup>3</sup>MC maps to have very little SMC emission. The “off” position observations were done very close in time to the mapping in order to take advantage of the mitigation of time variable rogue pixels and accurately capture the zodiacal light foreground. Subsequent removal of bad pixels was performed in Cubism.

In order to extract the spectrum of the remnant itself, it was necessary to remove local foreground and background emission from the observations. This was complicated by the location of E 0102 near the N 76 star-forming region which made foreground subtraction over a large area impossible. Instead we determined the local foregrounds in a ring surrounding the remnant with inner and outer radii of 30 and 50” , large enough to avoid subtracting emission that belongs to the remnant and small enough to well-represent the emission surrounding the supernova. In this ring we fit quartic surfaces to the emission at each wavelength and subtracted them from the spectral map. The modeled foreground/background emission appears very similar at most wavelengths except for near the strong [O IV] emission line near  $25.8 \mu\text{m}$ . At this wavelength there is a filamentary structure surrounding the remnant echoing that seen in optical [O III] images. This structure may be related to the nearby WR bubble in N 76 or may be the result of photoionization from the shock break out of the supernova.

### 3. The Mid-IR Spectrum of E 0102

The mid-IR spectrum of SNR 1E 0102.2 – 7219 is dominated by lines of highly ionized neon and oxygen and dust continuum. Figure 1 shows the background subtracted spectrum. An important consideration in determining the amount of dust that has formed in the remnant from the mid-IR spectrum is separating the contributions from forward-shocked circumstellar or interstellar dust, if present, from that of newly formed dust heated by the reverse shock. We use the spatial distribution of the emission lines and dust continuum compared with x-ray, radio and optical [O III] emission in the following section to argue for the presence of both newly formed dust and, most likely, some ISM/CSM dust in the mid-IR spectrum of E 0102.

The Chandra 0.3-10 keV x-ray image of the remnant shows a bright ring structure surrounded by a fainter plateau with a relatively sharp outer boundary (Gaetz et al. 2000). The bright ring is associated with reverse-shocked material and the outer plateau and edge marks the progress of the forward shock into the ambient medium. The ATCA 6 cm radio

image of the remnant also shows a ring structure, though the emission originates mainly in the outer region of the remnant, coincident with the x-ray plateau (Amy & Ball 1993). The radio emission originates in the forward-shocked ISM/CSM. Optical [O III] imaging of the remnant shows emission from the reverse-shocked ejecta, concentrated in the southern half of the remnant. Figure 2 shows a comparison of the optical [O III] image of the remnant from Blair et al. (2000) and images of the [Ne II] 12.8  $\mu\text{m}$  and [O IV] 25.8  $\mu\text{m}$  emission from our spectral map. The close correspondence of the distribution of the [Ne II] 12.8  $\mu\text{m}$  and [O IV] 25.8  $\mu\text{m}$  and the optical [O III] emission confirms that the infrared emission lines originate in the shocked ejecta as well. In Figure 3 we show stacked images of the dust continuum emission in two spectral regions with no ejecta emission lines. Both of the dust continuum images have a ring-like structure with bright spots in the lower half of the remnant.

At the resolution of the IRS observations, it is difficult to associate the ring morphology of the dust continuum emission with either the x-ray or radio emission. However, the enhanced emission from dust in the bottom half of the remnant shows that there is a dust component associated with the reverse-shocked ejecta. In the previous S<sup>3</sup>MC imaging of the remnant Stanimirović et al. (2005) noted the morphological similarity between the 24  $\mu\text{m}$  and x-ray emission, but it was unclear how much of the 24  $\mu\text{m}$  emission was due to the strong [O IV] line near 25.8  $\mu\text{m}$ . With our spectral maps we show that the correspondence of the dust continuum with the x-ray emission persists without the contamination of the [O IV] line, which only contributes around 10% of the 24  $\mu\text{m}$  flux. Therefore, we argue that the mid-IR emission from the supernova remnant is at least partially due to the emission from newly formed dust that has been heated by the passage of the reverse shock.

#### 4. Initial Results on the Dust Mass in SNR E 0102

Determining the mass of newly formed dust in SNR E 0102 is complicated by the possible presence of an ISM/CSM component and by our insensitivity to cooler dust. The S<sup>3</sup>MC 70 and 160  $\mu\text{m}$  images of the area are dominated by emission from the N 76 star-forming region and provide only an upper limit of 20 mJy at 70  $\mu\text{m}$ . In the mid-IR the dust we detect has been heated by the reverse shock. In the central part of the remnant, the dust, if it is present, is expected to be cold.

An interesting feature of SNR E 0102—observed at x-ray (Gaetz et al. 2000, Sasaki et al. 2006, Flanagan et al. 2004), optical (Tuohy & Dopita 1983), and now mid-infrared wavelengths—is that the chemical composition of the shocked ejecta is dominated by oxygen, neon and magnesium. This is in contrast to the younger remnant Cas A, which also shows emission from argon, sulfur and silicon in the mid-IR (Rho et al. 2008, Ennis et al. 2006).

This is interpreted as evidence that the reverse shock has only encountered the O-Ne-Mg layers of the progenitor star. The chemical composition of the unmixed ejecta determines the species of dust that can condense out of it (Kozasa et al. 1989, Nozawa et al. 2003). In the case of a  $25 M_{\odot}$  progenitor, the dust that condenses in the O-Ne-Mg layer of the ejecta is amorphous carbon,  $\text{Al}_2\text{O}_3$ , MgO and some silicates. In a future paper we provide more detailed modeling of the mid-IR spectrum (Sandstrom et al. 2008). As an initial estimate, we assume that all the mid-IR continuum is from newly formed amorphous carbon dust. Using the optical constants of Rouleau & Martin (1991) we find a best fit mass of  $5 \times 10^{-4} M_{\odot}$  of dust at a temperature of 110 K.

## 5. Conclusions

The initial results of our spectral mapping observations of SNR E 0102 indicate that the mid-IR spectrum contains a contribution from newly formed dust that has been heated by the reverse shock, most likely a component of CSM/ISM dust heated by the forward shock and highly ionized oxygen and neon in the supernova ejecta. We can establish the presence of newly formed dust by the spatial distribution of dust continuum compared to the emission lines. We find the [O IV] line at  $25.8 \mu\text{m}$  contributes  $\sim 10\%$  of the  $24 \mu\text{m}$  flux. We present an initial estimate of the mass of shocked, newly formed dust in the remnant of  $5 \times 10^{-4} M_{\odot}$ .

## REFERENCES

- Amy, S. and Ball, L., 1993, ApJ, 411, 761  
Blair, W. et al. 2000, ApJ, 537, 667  
Bolatto, A. et al. 2007, ApJ, 655, 212  
Chevalier, R., 2005, ApJ, 619, 839  
Dunne, L. et al., 2003, Nature, 424, 285  
Dwek, E. et al., 2007, ApJ, 662, 927  
Elmhamdi, A. et al., 2003, MNRAS, 338, 939  
Ennis, J. et al., 2006, ApJ, 652, 376  
Ercolano, B. et al., 2007, MNRAS, 375, 753  
Flanagan, K. et al., 2004, ApJ, 605, 230

Gaetz, T. et al., 2000, ApJL, 534, L47  
Houck, J. et al., 2004, ApJS, 154, 18  
Kozasa, T. et al., 1989, ApJ, 344, 325  
Krause, O. et al., 2004, Nature, 432, 596  
Meikle, W. et al., 2006, ApJ, 649, 332  
Meikle, W. et al., 2007, ApJ, 665, 608  
Nozawa, T. et al., 2003, ApJ, 598, 785  
Rho, J. et al., 2008, ApJ, 673, 271  
Rouleau, F. and Martin, P., 1991, ApJ, 377, 526  
Sandstrom, K. et al., 2008, in prep.  
Sasaki, M. et al., 2006, ApJ, 642, 260  
Smith, J. D. T. et al., 2007, PASP, 119, 1133  
Stanimirović, S. et al., 2005, ApJL, 632, L103  
Sugerman, B. et al., 2006, Science, 313, 196  
Tuohy, I. and Dopita, M., 1983, ApJL, 268, L11  
Wooden, D. et al. 1993, ApJS, 88, 477

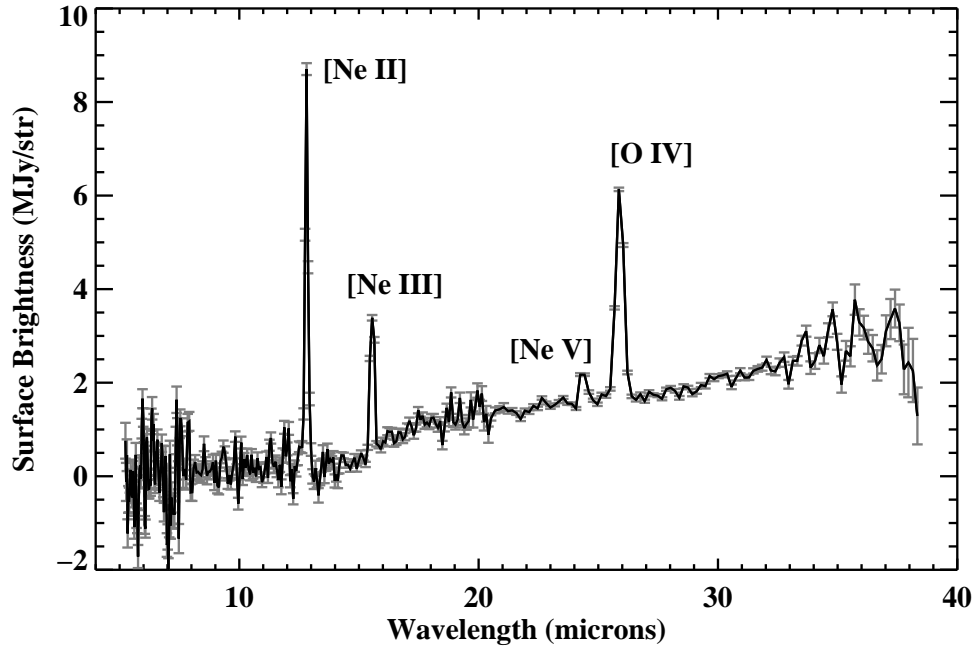


Fig. 1.— The background subtracted spectrum of SNR 1E 0102.2 – 7219.

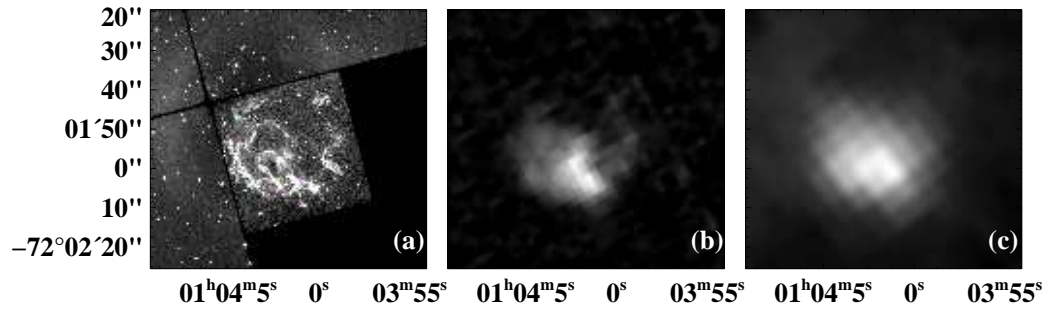


Fig. 2.— (a) [O III] image of E 0102 from Blair et al. (2000), (b) [Ne II] 12.8  $\mu\text{m}$  image, and (c) [O IV] 25.8  $\mu\text{m}$  image all at native resolution.



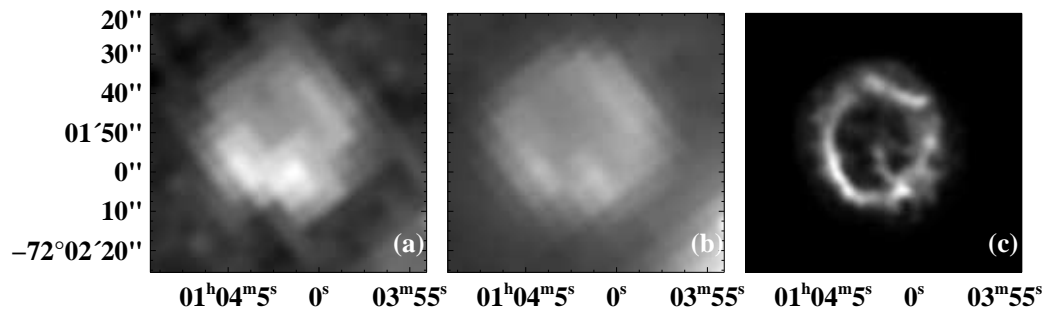


Fig. 3.— (a) 16.3 to 18.5  $\mu\text{m}$  dust continuum, (b) 27.5 to 31.7  $\mu\text{m}$  dust continuum and (c) Chandra 0.3-10 keV x-ray image from Gaetz et al. (2000) all at native resolution.